REPORT DOCUMENTATION PAGE

Form Approved
OMB No. 0704-0188

PLEASE DO NOT RETURN YOUR FORM TO THE ABOVE ORGANIZATION.

1. REPORT DATE *(DD-MM-YYYY)*	2. REPORT TYPE	3. DATES COVERED *(From - To)*
		1 MAR 07 - 30 NOV 09

4. TITLE AND SUBTITLE
Transition and transport in turbomachinery

5a. CONTRACT NUMBER

5b. GRANT NUMBER
FA9550-07-1-0183

5c. PROGRAM ELEMENT NUMBER

6. AUTHOR(S)
Paul Durbin

5d. PROJECT NUMBER

5e. TASK NUMBER

5f. WORK UNIT NUMBER

7. PERFORMING ORGANIZATION NAME(S) AND ADDRESS(ES)
Iowa State University

8. PERFORMING ORGANIZATION REPORT NUMBER

9. SPONSORING/MONITORING AGENCY NAME(S) AND ADDRESS(ES)
AFOSR
875 N Randolph Street
Arlington, VA 22203-1977

10. SPONSOR/MONITOR'S ACRONYM(S)

11. SPONSOR/MONITOR'S REPORT NUMBER(S)
AFRL-OSR-VA-TR-2012-0098

12. DISTRIBUTION/AVAILABILITY STATEMENT
A

13. SUPPLEMENTARY NOTES

14. ABSTRACT

The interaction of discrete and continuous Orr-Sommerfeld modes in a boundary layer is studied by computer simulation. The discrete mode is an unstable Tollmein-Schlichting wave. The continuous modes generate jet-like disturbances inside the boundary layer. Either mode alone does not cause transition to turbulence; however, the interaction between them does. The continuous mode jets distort the discrete modes, producing Lambda shaped vortices. Breakdown to turbulence is subsequent. The lateral spacing of the Lambda's is sometimes the same as that of the wavelength continuous modes, sometimes it differs, depending on the ratio of wavelength to boundary layer thickness.

15. SUBJECT TERMS

16. SECURITY CLASSIFICATION OF:			17. LIMITATION OF ABSTRACT	18. NUMBER OF PAGES	19a. NAME OF RESPONSIBLE PERSON
a. REPORT	b. ABSTRACT	c. THIS PAGE		12	Paul Durbin
					19b. TELEPHONE NUMBER *(Include area code)* (515) 294-7234

Reset

Final Report on AFOSR FA9550-07-0183

Paul A. Durbin

Aerospace Engineering, Iowa State University

---

1 Introduction

This project addressed the interaction between instability waves and Klebanoff modes for their relevance to compressors. It provided peripheral support to computer simulations of transition on compressor blades (see §5: Papers coming from this work). In light of the re-orientation of AFOSR university programs, I should note that the proposal was funded under Dr. Jeffries' program on turbomachinery and rotating flow.

It is generally believed that in turbomachines transition is via bypass mechanisms. There was a hint in the literature that on compressors instability waves might play a role. But that came from a good deal of filtering and wavelet transforming of a few transducer signals on a compressor rig. So we proposed to explore the topic at a basic level, under this AFOSR grant. We were quite surprised to find that the interaction between Klebanoff modes (the precursors to bypass transition) and Tollmein-Schichting waves (which are what is bypassed) could cause abrupt transition: discussed the following sections of this report. About the time of this grant we were initiating DNS of transition on a compressor geometry (most of the funding was via collaboration with colleagues at Univ. of Karlsruhe in Germany. Those simulations were carried over a couple of years and a last paper is only now under review). They confirm that the Klebanoff mode–TS interaction does indeed take place on compressor blades. This is contrary to the situation on turbine blades, and probably is influenced by the adverse pressure across a compressor.

The following summarizes some of the basic research done under this program. It is motivated, after the fact by the image in figure 1 from our DNS of transition on a compressor blade, beneath free-stream turbulence. That figure is showing a transition mechanism, in context. We started by studying the potential for such a process in the abstract, under AFOSR support.

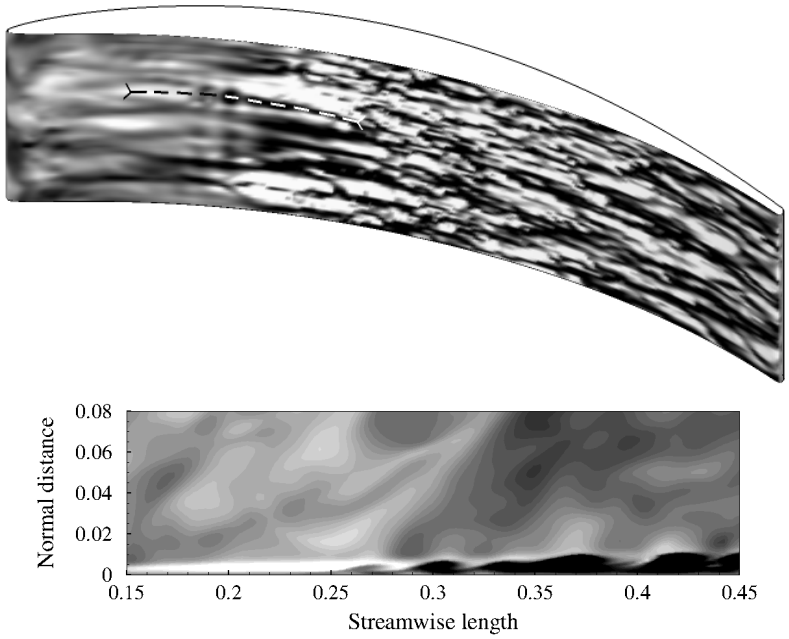

Fig. 1. *Plane and side views of the tangential perturbation field on DNS of a compressor blade. The dashed line marks the location of the side view (bottom pane). The side-view plane bisects a disturbance wave which leads to breakdown to turbulence.*

2 Simulations of the basic study

The numerical method for this study is a finite volume, staggered mesh, fractional step algorithm for the time-dependent, three-dimensional, incompressible Navier-Stokes equations in generalized coordinates. The spanwise direction is assumed to be periodic and is treated by spectral methods to reduce computational cost. The convective terms and the off-diagonal diffusion terms are advanced explicitly by the Adams-Bashforth scheme, while the remaining diffusion terms are treated implicitly by Crank-Nicolson. The Poisson equation for pressure is solved by line relaxation with multi-grid. The code is MPI parallel and simulations were performed on 32 processors of an AMD Opteron 280 cluster.

The inflow is specified as a superposition of a 3-D, spatially evolving continuous mode ($\hat{\boldsymbol{u}}_{con}$) and a 2-D spatially unstable Tollmien-Schlichting wave ($\hat{\boldsymbol{u}}_{TS}$) on a Blasius mean flow ($\boldsymbol{U}_b$):

$$\begin{aligned} u_0 &= U_b + Real\left[A_{con}\hat{u}_{con}(y)e^{-i\omega_{OS}t}\cos(k_z z) + A_{TS}\hat{u}_{TS}(y)e^{-i\omega_{TS}t}\right] \\ v_0 &= V_b + Real\left[A_{con}\hat{v}_{con}(y)e^{-i\omega_{OS}t)}\cos(k_z z) + A_{TS}\hat{v}_{TS}(y)e^{-i\omega_{TS}t}\right] \\ w_0 &= Real\left[A_{con}\hat{w}_{con}(y)e^{-i\omega_{OS}t)}\sin(k_z z)\right] \end{aligned} \qquad (2.1)$$

The Tollmien-Schlichting and continuous modes are obtained by solving the Orr-Sommerfeld and Klebanoff equations with well established methods: a Chebyshev collocation scheme is used to find the discrete modes and an implicit, matrix method is used for the continuous modes. The inflow T-S wave has a non-dimensional frequency

$$F \equiv \frac{\omega\nu}{U_\infty^2} 10^6 = 124.$$

At the inlet Reynolds number, $R_{\delta_{99}} = 2,000$, it is unstable and has a complex wavenumber

$$\alpha\delta_{99} = 0.6643 - 3.355 \times 10^{-3} i. \tag{2.2}$$

The inflow continuous O-S modes have non-dimensional frequency, wall-normal, and spanwise wavenumbers of

$$F = 33,\ k_y\delta_{99} = \pi/2,\ k_z\delta_{99} = n2\pi/L_z = nk_z^0 \tag{2.3}$$

The spanwise (z) wavenumber is expressed as a multiple of a wave number

$$k_z^0 = \frac{2\pi}{L_z}. \tag{2.4}$$

having period equal to the domain width. The domain width is eight times the initial boundary thickness, $L_z = 8\delta_{99}$. n is the number of waves spanning the domain. Hence, the physical scale of an n-wave inlet disturbance is $8\delta_{99}/n$. Results will be presented for $n = 2$ and $n = 5$ — which will be called mode 2, or long wavelength, and mode 5, or short wavelength. It should be emphasized that tests with a wider domain, and with these same wavelength disturbances, demonstrated domain independence. The relevant quantity is the wavelength $8\delta_{99}/n$, not the number of waves in the computational domain.

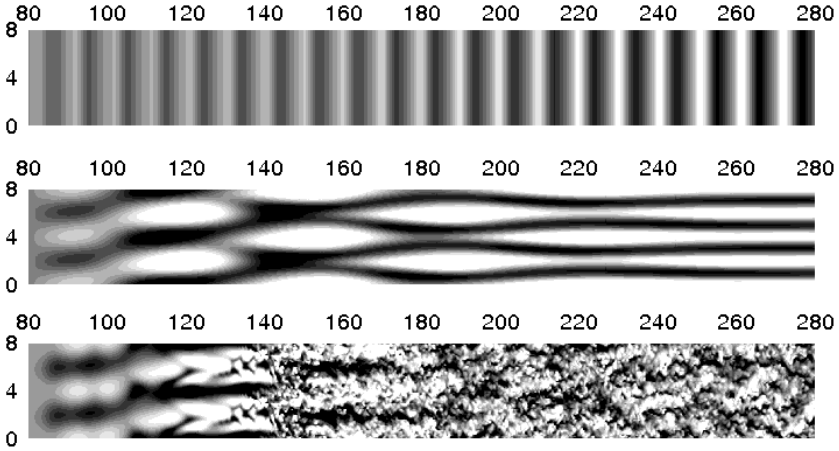

Fig. 2. Contours of fluctuating velocity of each mode alone: top pane, T-S wave; middle pane, continuous mode. Both modes are present in the lowest pane.

3 Results

Either mode, of itself, is unable to provoke transition. The two top panes of figure 2 contain contour plots of the T-S wave and the continuous mode 2 alone. The T-S wave grows exponentially, but remains two-dimensional. The continuous mode is three-dimensional, but stable. It induces a disturbance in the boundary layer, that evolves into a jet-like form: the velocity contours are elongated in the x direction and the dominant velocity component is u. Beneath free-stream turbulence, these jets are often termed streaks, or Klebanoff 'modes', or better, Klebanoff 'distortions'. The growth of streamwise elongated disturbances can be understood via linear theory. However, quadratic nonlinearity plays a role in the middle case of figure 2. The spanwise spacing of the contours is halved toward the end of the domain. This is caused by quadratic non-linearity acting on the initial spanwise periodicity. However, it is seen in the bottom pane of this figure that transition occurs before the wavelength has been halved.

With both modes present transition usually occurred within the computational domain. That is illustrated in the lowest plot of figure 2 and by figure 3. The later are skin friction curves comparing simulations with the unstable T-S wave alone, and with both modes present at the inlet. Lines presenting C_f versus R_x in laminar and in turbulent flow are included for reference. The average of the T-S wave alone case falls on top of the laminar line. With both modes present, the flow transitions, overshooting the turbulent line. That overshoot is typical of transition, although it can be exacerbated if the high demand for streamwise grid resolution once the boundary layer becomes turbulent is not fully met.

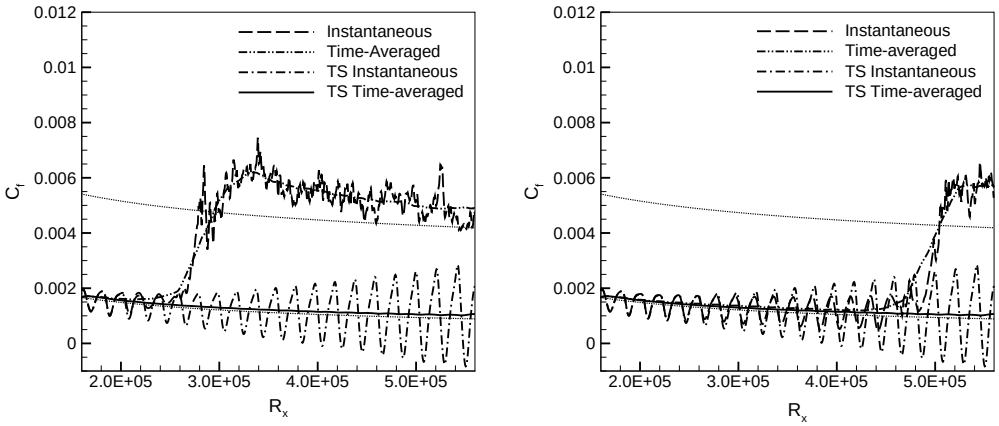

Fig. 3. The skin friction of modes 2 and 5. The discrete and continuous modes both have a 1% amplitude at the inlet.

The pattern of the perturbation when transition occurs is illustrated at the bottom of figure 2. Transition is preceded by the appearance of Λ shaped

velocity contours. Although this is reminiscent of secondary instability of Tollmien-Schlichting waves, the lateral spacing between Λ's is very much narrower and seems to be controlled by the spanwise mode number, n, of the continuous mode. Two broad classes of behavior were seen, as epitomized by modes 2 and 5 (c.f., equation 2.3). Those two cases are discussed in the next sections.

3.1 Long spanwise wavelength

A simulation with only the longer wavelength mode prescribed at the inlet is summarized in figure. The horizontal coordinate is measured relative to the inlet at $x_0 = 80$. Figure 4 looks down on a horizontal plane. The inlet Orr-Sommerfeld disturbance has the spanwise wavelength and streamwise periodicity of the continuous mode. Its non-linear evolution is illustrated by u contours.

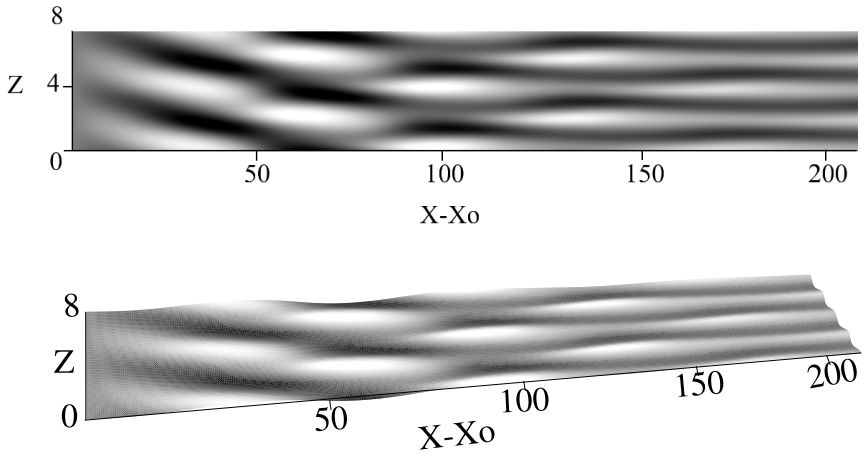

Fig. 4. Contours of streamwise fluctuating velocity in a horizontal cross sectional plane: mode 2.

The vertical sections in figure 5 show the Klebanoff response more clearly. The Orr-Sommerfeld mode is seen in the free-stream. Klebanoff modes are created inside the boundary layer. They distort the disturbance. Initially, the phase varies with height inside the boundary layer. The disturbance subsequently intensifies — each plane is scaled between its local maximum and minimum so that contours in the free stream become gray. Nonlinearity becomes apparent by $x - x_0 = 80$, as the spanwise wavelength begins to halve next to the wall. The cross-sectional planes show how the wavelength doubles from the wall, outward to the free-stream: near the top of the boundary layer the dark contours are seen to merge, forming an inverted 'v'.

By $x - x_0 = 170$ the boundary layer disturbance has become quite distinct from that in the free-stream. The lower image in figure 5 shows the variation

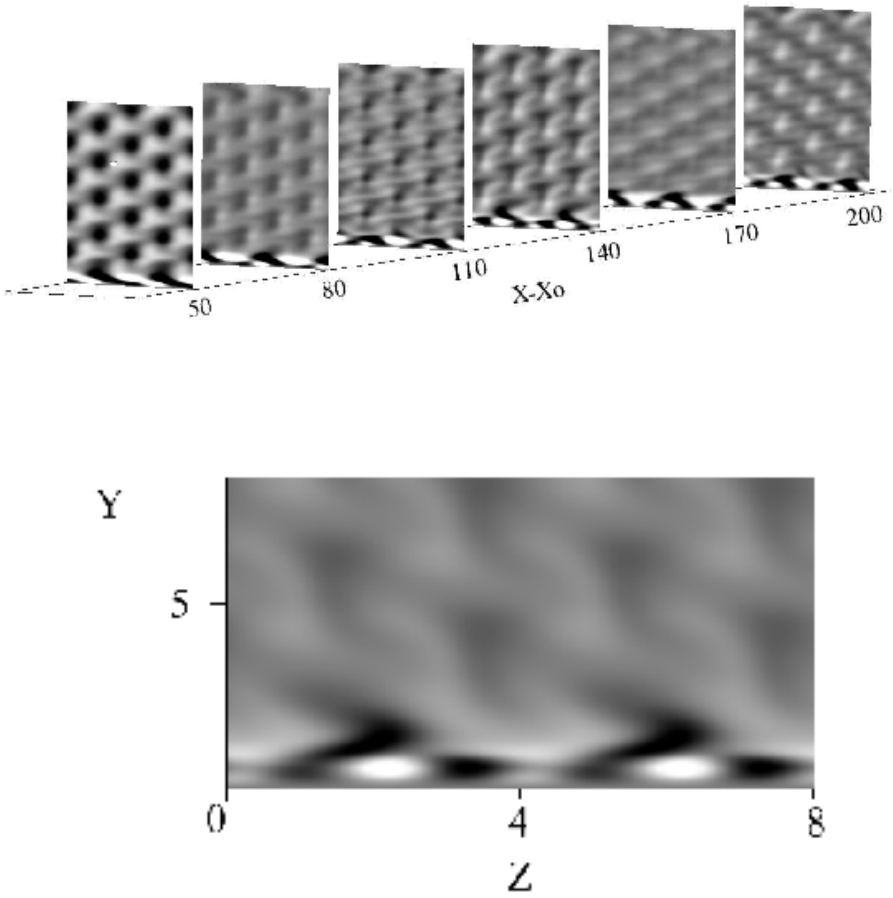

Fig. 5. Contours of streamwise fluctuating velocity in vertical cross sectional planes. The plane at $x - x_0 = 180$ is shown at the bottom.

of spanwise wavelength with height quite clearly.

Returning to figure 4, the wavenumber doubling is seen in the z spacing of the dark contours. The surface elevations in the lower part of the figure show how undulations in the x direction slowly decay, leaving a streamwise elongated disturbance. When the T-S wave is added to mode 2 at the inlet, transition occurs before the spanwise wavelength is halved, as will be seen shortly. The evolution of mode 2 far downstream is superseded by transition.

With both the continuous and the discrete mode present, transition occurs. Upstream of full transition to turbulence, velocity contours develop a Λ shaped pattern. The Λ's have a spanwise wavelength equal to that of the continuous mode.

Figure 6 is an instantaneous view of the perturbation field. It captures the early stages of development of a pair of Λ-structures at $x \sim 30$, and a mature pair further downstream, at $x \sim 38$. The Λ's are shaded by the mean velocity. Thereby, lighter gray indicates greater distance from the wall. The shaded surface is defined by $Q = -0.01$, where $Q \equiv \partial_i u_j \partial_j u_i$ is the difference between

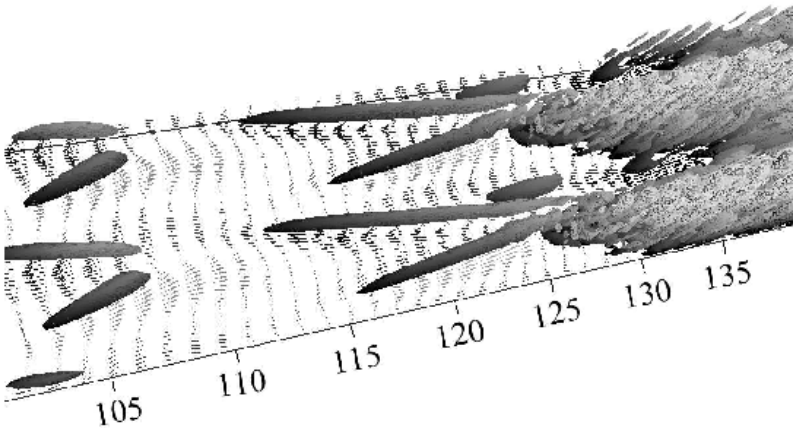

Fig. 6. Instantaneous disturbance showing the early stage of a pair of Λ structures, second pair downstream and breakdown to turbulence. Constant Q surface, shaded by mean velocity over velocity vectors in a plane.

rate of strain squared and rate of rotation squared. A region with $Q < 0$ is considered to identify a vortex. The constant Q surfaces show vortices lifting up, then breaking down into turbulence. Velocity vectors show both the jets caused by the continuous modes, and the flow induced by the vortices. These aspects will be pursued in subsequent figures.

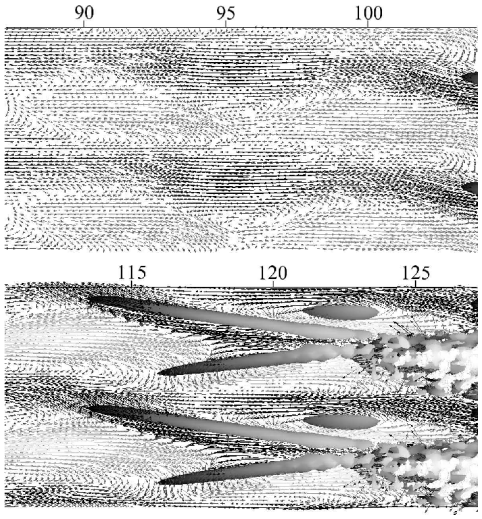

Fig. 7. Time sequence showing the inception of the Λ-structure, its growth, and finally breakdown. Smooth surfaces are the set $Q = -0.01$.

Figure 7 is a time sequence of the inception, growth, and breakdown of Λ-structures. Note that the viewing window translates downstream from frame to frame. Vectors show the in-plane perturbation velocity field. Light arrows represent forward velocities and darker shades indicate velocities that are negative relative to the mean flow. Constant Q surfaces cross the plane of velocity vectors. As previously, they are shaded by the mean velocity, so dark regions are near the wall.

Proceeding from the upper left, downward in the first snapshot a vortical region is observed near $x = 15$. In the second snapshot, this region becomes the inception point for a small vortex leg, which commences on a positive velocity perturbation (light vectors). A second leg emerges in the third snapshot, atop a region of negative velocity vectors. The gray scale shading shows that the vortices are lifting away from the wall, angled up from left to right.

The lightest shade of gray is near the outer edge of the boundary layer. In subsequent snapshots, the Λ vortices extend increasingly upward, reaching the top of the boundary layer as they convect downstream.

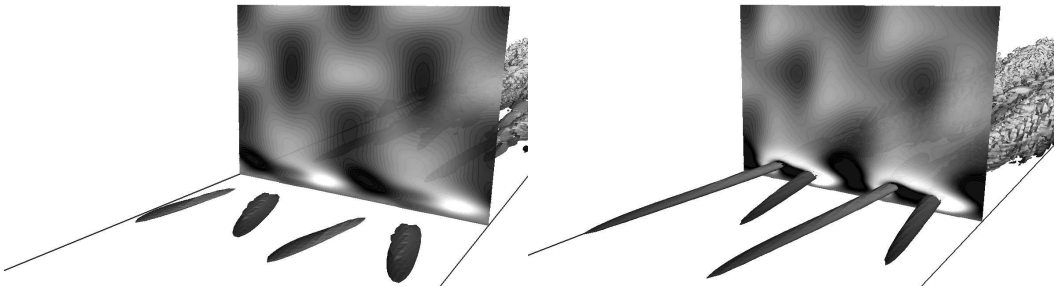

Fig. 8. The breakdown of the Λ structures. Time increases from upper left to lower right.

A clear asymmetry is captured in the time-sequence and is unique to this transition scenario (unlike the secondary instability of T-S waves in the absence of streaks). Despite emerging first, the lower leg, along the forward streak, is appreciably shorter than the upper leg. In the field of velocity vectors, vortical motion associated with the Λ's is only clear around the lower leg. The upper leg is significantly elongated due to the backward streak, which dominates the perturbation field in the plot of velocity vectors. The Λ's continue to stretch and lift away from the wall, and finally breakdown to turbulence at the lower right.

Figure 8 is a time sequence showing contours of u-perturbations in a cross-stream plane. The time instance in the top left pane is an early stage in the evolution of the Λ-structures. The cross-sectional plane is located downstream of the emerging vortices. The u velocity contours demonstrate that the boundary layer disturbance is, at this instant, still at the fundamental spanwise wavenumber. The incident continuous mode is apparent in the free-stream. Hence the wavenumber doubling, seen in figure 2, would occur further downstream, and is superseded by the modal interactions and transition to turbulence.

At all subsequent times, the cross-sectional plane is traversing the Λ's. A region of negative u-perturbation (dark contours) is observed between the two legs of the structure, and is contained within an originally forward (light contours) streak. This negative u-perturbation is induced by the vortical structure itself.

Circulation round the Λ shape causes upwelling in between the legs. This carries low-momentum fluid from the near the wall. Perhaps, it should be noted that, beyond the cross-sectional plane, the spanwise wavenumber of the continuous mode can be observed, even after breakdown to turbulence. Bands of turbulence emanate from the loop at the top of the Λ vortices. When the boundary layer becomes fully turbulent, the continuous mode wavelength is no longer evident (figure 2).

4 Students supported

Yang Liu, PhD: recieved 2008

Jongwook Joo, PhD: received 2008; then post-doc, partially on this grant

5 Papers coming from this work

Liu, Y., Zaki, T. & Durbin, P.A., 2008, Floquet Analysis of the Interaction of Klebanoff Streaks and Tollmien-Schlichting Waves, Phys. Fluids, 12, 124102

Liu, Y., Zaki, T. & Durbin, P.A., 2008, Boundary Layer Transition by Interaction of Discrete and Continuous Modes, J.Fluid Mech., 604, 199–233

Durbin, P.A., Zaki, T. & Liu, Y., 2009, Interaction of discrete and continuous boundary layer modes to cause transition, Int. J. Heat and Fluid Flow, 30, 403

Zaki, T., Wissink, J., Durbin, P.A. & Rodi, W., 2009, Direct computation of boundary layers distorted by migrating wakes in a linear compressor cascade, Flow Turbulence and Combustion, 83, 307

Zaki, T., Wissink, J., Rodi, W. & , Durbin, P.A., 2010, DNS of transition in a compressor cascade: the influence of free-stream turbulence, submitted JFM

Joo, J. & Durbin, P.A.2010 Approximate Decoupling of Continuous Modes and Mode Interaction in High-speed Boundary-layer Transition AIAA Journal, submitted

Conference presentations

Zaki, T.A., Liu, Y. Durbin, P. A& 2009 Boundary layer transition by interaction of streaks and Tollmien-Schlichting waves, IUTAM symposium on Laminar-Turbulent Transition

Durbin, P. A, Joo, J. & Marxen, O. 2008 Boundary Layer Transition in high-speed flow, Proceedings CTR summer program

Durbin, P. A, Liu, Y. & Zaki, T.A.. 2008 Boundary Layer Transition by Discrete and Continuous Modes, Engineering turbulence modelling and experiments (ETMM) VII

Zaki, T. A., Wissink, J., Durbin, P.A. & Rodi, W. 2008 DNS of wake-boundary layer interactions in a linear a compressor cascade, Engineering turbulence modelling and measurements (ETMM) VII

Wissink, J., Zaki, T. A., Rodi, W. & Durbin, P.A. 2008 Direct numerical simulation of flow in a low-pressure compressor cascade with incoming wakes WCCM8/ECOMAS 2008, Venice, Italy

Zaki, T. A., Durbin, P.A., Wissink, J. & Rodi, W. 2006 Direct numerical simulation of by pass transition in a linear compressor cascade ASME turbo expo., GT2006-90885